A new free-convection form to estimate sensible heat and latent heat fluxes for unstable cases

Francesc Castellví[1], Kosana Suvočarev[2,4], Michele L. Reba[3], Benjamin R.K. Runkle[4]

(1) Department of Environment and Soil Sciences, University of Lleida, Lleida, Spain. f-castellvi@macs.udl.cat.

(2) Department of Land, Air and Water Resources, University of California, Davis, CA, 95616, USA. ksuvocarev@ucdavis.edu

(3) USDA-ARS, Delta Water Management Research Unit, Jonesboro, AR 72401, USA. Michele.Reba@ARS.USDA.GOV

(4) Corresponding author. Department of Biological & Agricultural Engineering, University of Arkansas, Fayetteville, AR 72701, USA. brrunkle@uark.edu

Highlights:

- New Free Convection Limit approaches (FCL) are developed for turbulent fluxes
- FCL are tested over three surfaces of major interest in agriculture
- Similar surface energy balance closures obtained using FCL and reference methods

ABSTRACT

Free convection limit (FCL) approaches to estimate surface fluxes are of interest given the evidence that they may extend up to near neutral cases. For measurements taken in the inertial sublayer, the formulation based on surface renewal theory and the analysis of small eddies (SRSE) to estimate the sensible heat flux (H) was extended to latent heat flux (LE) with the aim to derive their FCL approaches. For sensible heat flux (H_{FCL}), the input requirements are traces of the fast-response (such as 10 to 20 Hz) air temperature and the zero-plane displacement. For latent heat flux (LE_{FCL}), input requirements are fast response traces of water vapor density, mean temperature of the air, the available net surface energy (Rn-G, where Rn and G are the net radiation and soil heat flux, respectively) and the zero-plane displacement. Taking eddy covariance (EC) as a reference method, the performance of the FCL method was tested over a growing cotton field that involved three contrasting surfaces: partly mulched bare soil, a sparse canopy and a homogeneous canopy. Using traces at 10 Hz and 20 Hz, H_{FCL} overestimated and underestimated the EC sensible heat flux (H_{EC}), respectively. In general, LE_{FCL} tended to slightly underestimate LE_{EC}. The surface energy balance closure show that (H_{EC} + LE_{EC}) underestimated (Rn-G) in a range of 19% (homogeneous canopy) and 8% (sparse canopy). Given that, in general (H_{FCL} + LE_{FCL}) was closer to (Rn-G) than (H_{EC} + LE_{EC}), the FCL method may be recommended for field applications, especially when the wind speed is not available.

KEYWORDS: Sensible heat flux; latent heat flux; surface energy balance; EC method; Free Convection limit

1. Introduction

The latent heat flux (LE) is involved in two fundamental equations, the surface energy-balance equation and the water-balance equation. Given that the main drivers for LE are the supply of water (including water content in topsoil) and the available net surface energy, (Rn – G) where Rn is the net radiation and G is the soil heat flux, it links hydrological, agricultural and climatological features (Dominguez et al., 2008; Li and Wang, 2019; Robles-Morua et al., 2012; Stagl et al., 2014; Yang and Wang, 2014). In particular, its knowledge is crucial for irrigation planning, to perform weather forecasting, climate modelling, to determine the risk of fire, among others (Brutsaert, 1982; Fang et al., 2018; Silva et al., 2010).

Direct measurements of LE by means of the eddy covariance (EC) method and large weighing lysimeters are preferred for scientific studies in agricultural landscapes. However, the required instrumentation and maintenance are expensive. When the sensible heat flux (H), LE and the available net surface energy are measured independently they allow calculating the simplified surface energy balance (Rn – G = H + LE), which can be used as a conventional quality control, to indirectly check the measurement reliability of H and LE (Aubinet et al., 2000). In general, the instrumentation required for monitoring LE over large areas involving different surfaces is not always affordable or applicable (Haymann et al., 2019) and, on the other hand, flow distortion and windy conditions (among others) are problems when using, respectively, the EC method and a weighing lysimeter (Alfieri et al., 2012; Brutsaert, 1982; Burba, 2013; Noltz et al., 2013). Thus, techniques and approaches to estimate LE are of interest to overcome some shortcomings in measurement scaling and cost that are inherent in the EC method and weighing lysimeters (Albertson et al., 1995; Castellví, 2004; Drexler et al., 2004 and 2008; French et al., 2012; Haymann et al., 2019; Li and Wang, 2019; Paw U et al., 1995; Snyder et al., 1996; Suvočarev et al., 2019; Yang and Wang, 2014; Zhao et al., 2010).

To minimize costs, in moderately tall canopies LE has often been estimated indirectly using the simplified energy balance residual method (i.e., LE = Rn – G – H) because the instrumentation required to estimate H, G and Rn is more affordable. A major (potential) issue involved in the residual method to estimate LE half-hourly is that accurate measurements of all the energy terms involved in the surface energy balance (SEB) equation do not guarantee its closure. On a half-hourly basis, in general, even on extended homogeneous surfaces, the sum of turbulent fluxes is smaller than the available net surface energy (Foken 2008; Foken et al., 2011; Twine et al., 2000; Wilson et al., 2002). Thus, often the residual method adds unexplained energy to LE. There is an ongoing scientific debate about the role of low frequency circulations in the lack of closure of the SEB equation (Cuxart et al., 2015; Eder et al., 2014; Foken, 2008; Huang et al, 2008; Kanda, 2004; Stoy et al., 2013; Steinfeld et al., 2007). While some studies have suggested that large circulations appear to be more efficient in transporting sensible heat than latent heat (Charuchittipan et al., 2014; Stoy et al., 2006 and 2013), other studies have shown that this role depends on the surface heterogeneity, type of terrain, and its uses (Brunsell et al., 2011; Cuxart et al., 2015). These issues may affect the uncertainty when the residual method to estimate LE is used. In fact, at some sites the residual method may be preferred to estimate H (i.e, H = Rn – G – LE) than LE (Castellví and Oliphant, 2017).

When the Monin – Obukhov Similarity Theory (MOST) is used, through the stability parameter, the friction velocity (u_*) and the sensible heat flux are required as input to estimate the latent heat flux. Traditionally, to avoid measurement of the wind field, the wind log-law is implemented to estimate u_*, H and LE (Castellví and Snyder, 2008; De Bruin et al., 1993; Hsieh et al., 1996; Suvočarev et al., 2019). When convection dominates the turbulence in the atmospheric surface boundary layer, MOST similarity relationships were redone to best fit this limit case (termed free convection limit, FCL, approaches) (Stull, 1988). Implementing the FCL formulation, surface eddy flux estimates of scalars become independent of the friction velocity. Consequently, FCL approaches become simpler and, surprisingly, there is evidence that they performed rather reliably up to near-neutral conditions (Albertson et al., 1995; Högström, 1988; Kohsiek, 1982; Monin and Yaglom, 1971; Wang and Brass, 2010). For field applications, minimization of input requirements has special interest when surface flux estimates are desired at multiple sites, such as in the framework of remote sensing and estimation of crop coefficients (Drexler et al., 2008; French et al., 2012; Zapata and Martínez-Cob 2001; Zhao et al., 2010).

The framework of Surface Renewal (SR) theory (Danckwerts, 1951; Harriot, 1962; Higbie, 1935; Seo and Lee 1988), combined with the analysis of Small Eddies (SRSE) (Aminzadeh, 2017; Castellví, 2018; Haghighi and Or, 2013 and 2015), has shown potential to open new perspectives in micrometeorology. For instance, an SRSE approach was proposed to estimate u_* (alternative to the wind log-law) and H requiring as input measurements of the mean wind speed and the high-frequency trace of the air (or virtual) temperature in the roughness and inertial sub-layers (Castellví, 2018). In the following, the SRSE formulation will refer to applications requiring measurements taken in the inertial sub-layer as input and it will be used to estimate LE. To our knowledge, the SRSE approach to estimate fluxes of scalars other than temperature, has never been tested. Here, given the benefits of developing approaches requiring minimum inputs, an SRSE-FCL expression was derived for estimating H and LE. It was shown that the inputs required to determine H as H_{FCL} are fast-response traces of air temperature and the zero-plane displacement. Similarly, for LE, LE_{FCL} may be determined using fast-response traces of water vapor concentration, the zero-plane displacement, the mean temperature of the air and the available net surface energy as input. Therefore, H_{FCL} and LE_{FCL} do not share instrumentation. This separation minimizes the probability to have simultaneous gaps in H and LE. In addition, H_{FCL} and LE_{FCL} are estimated independently which allows testing closure of the surface energy balance for an integral quality check. Here, the performance of H_{FCL} and LE_{FCL} were tested for a growing cotton field, which involved surfaces with different roughness.

2. Theoretical considerations

2.1 The SRSE method with measurements in the inertial sub-layer

SRSE is a semi-empirical method, fully described in Castellví (2018), to estimate the friction velocity and eddy fluxes. To estimate the surface flux of a scalar, SRSE considers that downward flows (i.e., descending macro-parcels of air following a coherent motion) generate a narrow, highly turbulent, shear layer containing multiple small-scale vortices (Zhu et al., 2007). SRSE assumes: (1) the population of small eddies (which in the following are termed fluid elements) generated in the volume within the canopy of the macro-parcel are randomly distributed; (2) during the time that a fluid element remains close to the viscous sub-layer of a source (exposure time), mass and heat transfers through and the fluid element increases (or depletes) its scalar concentration until it is randomly replaced by another fluid element; (3) by continuity, following the coherent motion, the macro-parcel remains in contact with the surface for a given period (though it depends on the wind speed, surface roughness and stability conditions, this period is on the order of a few tens of seconds) until it ejects being renewed by a new sweep (Katul et al., 1996; Paw U et al., 1995; Zhu et al., 2007). During ejection most fluid elements located in the upper part of the canopy remain attached to the macro-parcel of air (Zhu et al., 2007). As a consequence, regularly (i.e., at the sweep – ejection frequency) a large number of fluid elements are broadly spread above the canopy in the surface boundary-layer (Katul et al., 1996; Zhu et al., 2007). Additionally, SRSE assumes (4) the coherent motion transports fluid elements across finite distances before they have a chance to be dissipated or become significantly diluted. Thus, a transilient turbulence mixing concept is adopted (Stull, 1984).

For an unstable case, Fig. 1 depicts the formation and identification of the fluid elements. It shows a macro-parcel of air (defined as a parcel of air whose volume covers most sinks and sources) following a coherent motion (Fig. 1, panel a). The actual trace of the sonic temperature and water vapor concentration of the air (measured at 20 Hz on May 5 at 17.5 h) for a short interval is shown in Fig. 1 (panel b) which was composed by small fluctuations (signatures of fluid elements) embedded in the scalar change of a macro-parcel of air over time (t) (signature of a coherent structure). In Fig. 1 (panel b), the signature of the coherent structure was assumed to follow the generalized ramp-like shape (Fig. 1, panel b) proposed in Chen et al. (1997a) which is composed by three phases (quiescent, enriching and ejection). Regardless, the composition shown in Fig. 1 admits any ramp model to identify coherent motions (Chen et al., 1997a; Paw U et al., 1995; Shapland et al., 2012; Van Atta, 1977) because in the SRSE method the analysis to identify coherent motions is bypassed. The SRSE method focuses on the fluid elements attached to macro-parcels of air whose frequencies are in the order of tenths of a second. For a given trace of scalar (s), where in the following $\underline{s}$ may refer either to virtual temperature or temperature of the air (T) and to water vapor concentration (W), the exposure time for an i^{th}-fluid element (τ_{is}) was estimated as the time between two consecutive valleys in the trace and its net scalar increase (a_{is}) as the difference between the value achieved at the peak and at the first valley. As an example, Fig. 1 (panel c) shows two fluctuations for sonic temperature and one for water vapor concentration. For the latter, the time exposure and amplitude were 0.2 s and 0.3 g m^{-3}, respectively.

To estimate the sensible heat flux carried out by a fluid element, SRSE assumes (Castellví, 2018): (1) a fluctuation follows a ramp-like shape whose quiescent period can be neglected because the mass of a fluid element is small (Fig. 1, panel c) and; (2) the eddy diffusivity for heat (K_{hi} where i denotes the i^{th} fluid element) is mainly driven by shear and can be parameterized as $K_{hi} = k\ \tau_{iT}(u_i'w_i')$ where u_i' and w_i' denote fluctuation (Reynolds decomposition) of the horizontal and vertical wind speed, respectively. Given that $(u_i'w_i')$ represents a portion of the mean friction velocity which weight is expected to depend on the size of the fluctuation, a semi-empirical relationship for $\frac{K_{hi}}{\tau_{iT}}$ was proposed weighting each fluctuation by the ratio of the time exposure over the mean time exposure of fluid elements as, $\frac{K_{hi}}{\tau_{iT}} = k\frac{\tau_{iT}}{\bar{\tau}_T}\phi_{h(\varsigma)}^{-1}u_*^2$ (where k is the Von Kármán constant, $\bar{\tau}_T$ is the averaged time exposure of all fluid elements in half an hour temperature trace, ϕ_h is the stability function for the heat transfer and $\varsigma\left(=\frac{Z-d}{L}\right)$ is the stability parameter; Z is the measurement height, d is the zero-plane displacement and L is the Obukhov length).

Here, to estimate the latent heat flux carried out by a fluid element it was assumed that the eddy diffusivity for water vapor of the *i-th* fluid element (K_{wi}) over its time exposure follows the same analytical form as for temperature. Therefore, K_{wi} was parameterized as, $\frac{K_{wi}}{\tau_{iw}} = k\frac{\tau_{iw}}{\bar{\tau}}\phi_{w(\varsigma)}^{-1}u_*^2$ where $\phi_{w(\varsigma)}^{-1}$ is the stability function for the transfer of water vapor. For the i^{th} fluid element, K_{hi} and K_{wi} are expected to be different because time exposures for air temperature and water vapor are different (i.e., the flux-footprint area of each source, such as a leaf, is different for a given scalar). An example of this difference is in Fig. 1 (panel c).

2.2. Sensible heat flux

When the turbulent diffusion equation is solved for the i^{th} fluid element with an eddy diffusivity for heat over time exposure, $\frac{K_{hi}}{\tau_{iT}} = k\,\frac{\tau_{iT}}{\bar{\tau}_T}\,\phi_{h(\varsigma)}^{-1} u_*^2$, its sensible heat flux density (H_i) can be expressed as (Castellví, 2018)

$$H_i = \rho c_p \sqrt{\frac{k}{\pi}}\;\; \phi_{h(\varsigma)}^{-1/2} u_* \left(\frac{\tau_{iT}}{\bar{\tau}}\right)^{1/2} a_{iT} \tag{1}$$

where ρ and c_p are the density and isobaric specific heat capacity of the air, respectively. Here, we note that because Eq. (1) refers to a fluid element, the small volume of the parcel (ΔV_i) to consider for this eddy may be written as $\Delta V_i = S\, dZ_i$ where S denotes a unit area and dZ_i represents a small part of the total vertical extent of fluid elements ejected up to the measurement height. To determine the total sensible heat flux, the sensible heat flux carried out by the fluid element obtained after averaging Eq. (1) for all the time exposures (i.e., a representative fluid element of the population) must be integrated to account for all the volume (per unit area) containing fluid elements. Hence, the mean flux of sensible heat injected to the surface sub-layer by the macro-parcel of air can be estimated as

$$H_{Est} = \frac{Z_V}{N\,\bar{\tau}} \sum_{i=1}^{i=N} H_i\, \tau_{iT} = Z_V \frac{\rho c_p \sqrt{\frac{k}{\pi}}}{N\,\bar{\tau}}\;\; \phi_{h(\varsigma)}^{-1/2} u_* \left(\sum_{i=1}^{i=N} \left(\frac{\tau_{iT}}{\bar{\tau}}\right)^{1/2} \tau_{iT}\, a_{iT} \right) \tag{2}$$

where Z_V (dimensionless) accounts for the volume of air containing fluid elements (V_c) per unit volume (i.e., $Z_V = \frac{\mathrm{Vc}}{1\,m^3}$ represents the total vertical extend of fluid elements ejected up to the measurement height per unit height) and N is the total number of fluid elements observed in half an hour, thus $N\,\bar{\tau}$ = 1800 s. The theoretical Probability Distribution Function (PDF) of time exposures proposed in Seo and Lee (1988) involves a coefficient (α) that accounts for the spectra of fluid elements.

It was found that the theoretical PDF can explain the actual PDF observed within and above the canopy (Castellví, 2018) and that from the top of a canopy down to a height of about 2/3 the canopy height the profile of α showed a decay similar to the mean wind speed. From the ground up to about 2/3 the canopy height, the α profile was unpredictable. Therefore, by assuming codependence between the distinct turbulent flows near and far from the surface (Haghighi et al., 2013), the predictable α dependence on height was interpreted as representing that the majority of fluid elements sampled at the measurement height were placed above the zero-plane displacement during the ejection phase. This assumption was partly supported by Zhu et al. (2007) who showed for a homogeneous canopy that most of the fluid elements that spread above the canopy during the ejection phase originated in the upper part of the canopy. Additionally, sensible heat fluxes estimated setting $Z_V = p_v(Z - d)$ in Eq. (2) with $p_v = 1\, m^{-1}$ and $p_v = f_c\, m^{-1}$ (where f_c is the fraction of ground canopy cover) for homogeneous and sparse canopies, respectively, compared close to H_{EC} (the reference). For completeness (i.e., to include bare soil or surfaces where bare soil dominates over sparse short vegetation), here it is proposed to estimate Z_V setting $p_v = 0.5\, m^{-1}$ which is empirical (supported in Sect. 4.1.2). This case assumes that the fluid elements mainly originated in the bottom part of the macro-parcel. Therefore, Z_V is expressed as

$$Z_V = p_v \begin{cases} (Z - d) & homogenous\ canopy \\ (Z - d) f_c & sparse\ canopy \\ 0.5\, Z & bare\ soil \end{cases} \quad (3)$$

Where here, p_v is set to 1 m^{-1} for dimensional homogeneity. The bare soil case seems to introduce a discontinuity in Z_V, but it does not because the bare soil must be interpreted as a different interface (i.e., coherent structures penetrate into the canopy, but the ground acts as a wall).

2.3. Latent heat flux

On the basis of the K_{hi} and K_{wi} parameterization (Sect. 2.1) and assuming that the stability functions are similar regardless of the scalar (i.e, $\phi_{w(\varsigma)}^{-1} = \phi_{h(\varsigma)}^{-1} = (1 - 16\,\varsigma)^{0.5}$, Dyer (1974)), the analytical form for the sensible heat flux is valid for any scalar (Castellví, 2004 and 2013). Therefore, the latent heat flux can be estimated as

$$LE_{Est} = Z_V \frac{L_v}{N\,\bar{\tau}} \sqrt{\frac{k}{\pi}}\ \phi_{h(\varsigma)}^{-1/2} u_* \sum_{i=1}^{i=N} \left(\frac{\tau_{iw}}{\bar{\tau}}\right)^{1/2} a_{iw}\ \tau_{iw} \qquad (4)$$

where L_v is the heat of vaporization and Z_V is estimated by Eq. (3).

2.4 Free convection approaches

2.4.1 Sensible heat flux

For unstable cases, the stability function for the transfer of momentum $\phi_{m(\varsigma)}$ and heat are related as, $\phi_{h(\varsigma)} = \phi_{m(\varsigma)}^2$. The free convection form for $\phi_{m(\varsigma)}$ is $\phi_{m(\varsigma)} = 0.42\,(-\varsigma)^{-1/3}$ for $\varsigma \leq -0.16$ (Högström, 1988) which can be combined with Eq. (2) and the Obukhov length $L\ (= -{u_*}^3 \left(\frac{kg}{T}\frac{H}{\rho C_p}\right)^{-1}$, where g is the acceleration of gravity and T the mean air temperature) to estimate the half-hourly free convection limit sensible heat flux as

$$H_{FCL} = Z_V^{3/2} \rho C_p \left(\frac{k}{\pi}\right)^{3/4} \left(\frac{1}{0.42}\right)^{3/2} \left(\frac{kg(Z-d)}{T}\right)^{1/2} \left[\frac{1}{N\,\bar{\tau}}\left(\sum_{i=1}^{i=N}\left(\frac{\tau_{iT}}{\bar{\tau}}\right)^{1/2} \tau_{iT} a_{iT}\right)\right]^{3/2} \qquad (5)$$

2.4.2 Latent heat flux

Combining Eq. (4), the FCL form for $\phi_{h(\varsigma)}$, the Obukhov length and the SEB equation to estimate H (i.e, H = Rn – G – LE), the following 3*rd* order equation involving the free convection limit approach for the latent heat flux is obtained

$$\mathrm{LE}_{FCL}{}^{3} + b_u\,\mathrm{LE}_{FCL} - b_u\,(\mathrm{Rn} - \mathrm{G}) = 0 \qquad (6)$$

where the coefficient b_u is positive

$$b_u = Z_V^3 \left(\frac{L_v}{0.42}\right)^3 \left(\frac{k}{\pi}\right)^{3/2} \left(\frac{kg(Z-d)}{\rho C_p T}\right) \left[\frac{1}{N\,\bar{\tau}} \left(\sum_{i=1}^{i=N} \left(\frac{\tau_{iw}}{\bar{\tau}}\right)^{1/2} \tau_{iw} a_{iw}\right)\right]^3$$

3. Materials and methods

3.1. The field campaign

From 13 May to 30 September 2016, an experiment was carried out on a cotton field in Manila, AR, US (35° 53' 14", −90° 8' 15") (Suvočarev et al., 2019; Fong et al., 2020). The field was on a flat terrain (0.1% slope), the crop was sprinkler irrigated, and the fetch, in practice, may be considered unlimited regardless of the wind direction because the flux tower was deployed between two fields of the same cotton crop (63×10^4 and 45×10^4 m^2). From the beginning of the campaign up to 22 June, bare soil dominated the field. Sparse mulches made of the cover crop residues (about 0.1 m thick) remained and the fraction of ground cover was about 30%. Sparse vegetation predominated from 22 June to 18 July and during this period the canopy height (h_c) and the fraction of ground cover varied from about $h_c = 0.25$ m and $f_c = 30$ % up to about $h_c = 0.90$ m and $f_c =$ 85%, respectively. After 18 July the crop was considered homogeneous, f_c remained about 85%, and the maximum canopy height, $h_c = 1.10$ m, was reached around 28 July. A three dimensional (3-D) sonic anemometer (CSAT3) and a gas analyzer (LICOR, 7500A) operating at 20 Hz were deployed at Z = 3 m.

The net radiation (CNR4, Kipp and Zonen) was measured at 2 m above the ground and other conventional measurements were performed to estimate the soil heat flux at three points located about 8 m into the North field. At each point, G was determined summing the heat flux at 0.08 m below the ground and the ground heat storage above the soil heat flux plate (Fuchs and Tanner, 1968; Sauer and Horton, 2005). The heat flux was measured with a flux plate (HFP01SC, Hukseflux) placed 0.08 m below the ground. The change in heat storage in the soil above the plate was estimated using the calorimetric method (Fuchs and Tanner, 1968). Changes in soil temperature were measured using a temperature probe (107, Campbell Scientific) placed above the soil heat flux plate at 0.06 m below the ground surface and the volumetric water content was measured with a Digital Time Domain Transmissometer (Digital TDT soil moisture sensor, Acclima) adjacent to the flux plate. For water, the specific heat capacity and density were set to 4.19 kJ kg^{-1} K^{-1} and 1 kg m^{-3}, respectively. For dry soil, the specific heat capacity was 0.9 kJ kg^{-1} K^{-1} and the bulk density was 1470 kg m^{-3}.

3.2. Method and performance evaluation

3.2.1 Database

The entire dataset was split into three sub-datasets referred to as bare soil, sparse-canopy, and homogeneous-canopy datasets with samples collected from the beginning of the experiment up to 22 June, from 23 June up to 18 July, and from 19 July up to the end of the experiment, respectively. For each half an hour, regardless of the dataset, two traces were formed; one sampling the measurements at a frequency of 10 Hz and another at 20 Hz. The former was obtained by down-sampling (i.e. skipping every other 0.05 s sample in the original 20 Hz series). Therefore, the impact in H and LE estimates when different sizes of fluid elements are resolved was compared. For field applications, this is of main interest with regard to using thicker fine-wire thermocouples (i.e., that are more robust) to measure the temperature of the air and saving space in memory cards. For the bare soil dataset, (Rn-G) was available for a total of 117 half-hourly samples due to damage and power issues at the beginning of the campaign.

3.2.2 Canopy parameters

The zero-plane displacement was neglected for the bare soil dataset because the fraction of canopy cover was small and the mulch and vegetation at tillering were short and sparse. For the other two datasets, it was estimated as $d = 2/3h_c$ (Brutsaert, 1982). The sparse canopy dataset was split in three sub-periods of about 10 days each because the crop was growing. Intermediate values for the pair (h_c, f_c) for each sub-period were (0.4 m, 0.4), (0.6 m, 0.6) and (0.8 m, 0.8), respectively. For the homogeneous dataset, the intermediate pair was (1.05 m, 0.85).

3.2.3 Post-field flux processing and performance evaluation

After correcting the wind field for flow distortion due to transducer shadowing (Horst et al., 2015) and removing samples where mean streamwise directions approached the back of the sonic anemometer (by ± 30° to avoid flow distortion by the tower mounting), EC sensible and latent heat fluxes, H_{EC} and LE_{EC}, respectively, were determined using the package EddyPro 6.2 (LI-COR Biosciences, Lincoln, NE) with time series at 20 Hz. Samples were filtered for positive H_{EC} and those that accomplished 90% fetch from the observed field.

Regardless of the scalar, time exposures and amplitudes for each fluid element in a 30 min scalar trace were determined analyzing the fluctuations observed (Fig. 1, panel c). Thus, for a given fluctuation (signature of a fluid element) in sonic temperature or water vapor concentration traces, the time exposure and amplitude was determined as the time between two consecutive *valleys* and the difference between the peak and the first valley, respectively (Castellví 2018). According to the SEB equation for unstable cases, LE_{FCL} was solved by minimizing Eq. (6) with boundaries $0 \leq LE_{FCL} \leq (Rn\text{-}G)$. Once LE_{FCL} was obtained, the traces of sonic temperature were used to estimate the buoyant heat flux using Eq. (5) and the final H_{FCL} was determined after humidity correction (Schotanus et al., 1983). The performance of H_{FCL} and LE_{FCL} was compared against the EC method and discussed in relation to their capability in closing the SEB equation, (H+LE) versus (Rn-G). Comparisons were performed by calculating the slope, the intercept, the coefficient of determination (R^2) of the linear regression analysis, a normalized root mean square error (NRMSE) which was calculated as the RMSE over the mean flux taken as a reference (i.e. the corresponding EC flux in this case), and the mean bias error (MBE) which is defined as $MBE = \frac{1}{N}\sum_{i=1}^{i=N}(y_{i\,est} - y_i)$ where y_{est} and y denote the estimated and the measured reference variable, respectively. Moreover, H_{Est} and LE_{Est} were included in the comparison which involve the stability parameter. Here, approaches to estimate the stability parameter when the sonic anemometer is not available were omitted (i.e., the focus is the FCL formulation which does not involve the stability parameter) and, in a straightforward manner, it was determined using as input the friction velocity and the buoyant heat flux from the sonic anemometer high frequency measurements.

4. Results and discussion

4.1 Results

For each dataset, Table 1 shows the regression characteristics and model error terms to compare H and LE determined using traces of scalars sampled at 10 Hz against the corresponding EC reference fluxes, and (H+LE) against (Rn-G). The results obtained for H and LE determined using the sampling frequency of 20 Hz differed from the results obtained at 10 Hz are shown in parentheses. Though not shown in Table 1, for each half-hour scalar trace the number of fluid elements resolved at 20 Hz nearly doubled those resolved at 10 Hz. Thus, the different performance shown in Table 1 would partly be related to the amount of small eddies resolved. As an example of an indirect quality control for eddy fluxes determined using the EC and FCL methods, Fig. 2 shows a comparison between (H_{EC}+LE_{EC}) and (H_{FCL}+LE_{FCL}) determined using scalar traces sampled at 10 Hz versus (Rn-G) for each dataset.

4.1.1 Sensible heat and latent heat fluxes

Regardless of the dataset, sampling frequency and method to estimate H and LE, Table 1 shows that the intercepts (int) were small and that the MBE values nearly fall within the accuracy of determining H_{EC} and LE_{EC} using different brands of sonic anemometers (Foken, 2008; Foken and Oncley, 1995).

Regardless of the dataset and the method to estimate H and LE, the estimates determined using traces at 10 Hz were in general slightly better correlated with the EC method than using traces at 20 Hz. In any case (i.e., regardless of the frequency), the coefficients R^2 for H and LE were high (the minimum R^2 was 0.80). The slopes obtained show that the H and LE estimates determined using traces at 10 Hz consistently overestimated those calculated using traces at 20 Hz. For sensible heat flux the overestimation was about 30%. For latent heat flux, the overestimation depended slightly on the surface. Regardless of the method, it was about 18% and 15% for the bare soil and the sparse-canopy datasets, respectively. For the homogeneous dataset, LE_{Est} compared higher (about 25%) than using LE_{FCL} (about 10%). Given the generalized small intercepts and MBE values and the high coefficients R^2, the performance in the slopes lead, in general, to higher NRMSE values at 10 Hz than at 20 Hz.

Regardless of the dataset and the sampling frequency, the main difference between the SRSE methods to estimate the sensible heat flux was that H_{FCL} correlated slightly better to the EC method than H_{Est} and the intercepts were slightly smaller using H_{FCL} than H_{Est}. H_{FCL} also generated smaller NRMSE values than H_{Est} and, in general, to slightly smaller MBE values. For latent heat flux, the only one clear pattern observed comparing the two SRSE methods was that the NRMSE values obtained using LE_{FCL} were smaller than using LE_{Est}. The other statistics were similar.

4.1.2 Surface energy balance

Regardless of the dataset and the SRSE method, the slopes comparing the total turbulent flux to the available net surface energy estimated using scalar traces at 10 Hz were slightly closer one than using scalar traces at 20 Hz. The intercepts were, in general, closest to zero at 20 Hz than at 10 Hz. Coefficients R^2, NRMSE and MBE values did not show dependency on the sampling frequency.

In general, the SRSE and EC methods generated a similar surface energy balance closure. In fact, the EC method was not consistently superior to SRSE and, on the basis of NRMSE, the FCL method operating at 10 Hz was the best. For each surface, Fig. 2 shows that (H_{FCL}+LE_{FCL}) and (H_{EC}+LE_{EC}) scattered around (Rn-G) similarly, including in near neutral cases. Thus, the extension of the FCL approach to small values of the stability parameter leads to a performance similar to the EC surface energy balance closure.

For bare soil, (H_{Est}+LE_{Est}) and (H_{FCL}+LE_{FCL}) were highly correlated with (Rn-G) which suggests that for this surface a refinement of the parameter p_v, or coeficient 0.5 in Eq. (3), would close the surface energy balance better, especially for the FCL method. In practice, a coefficient obtained by forcing closure of surface energy balance could be interpreted as the factor, instead of 0.5, required in Eq. (3). However, it is not clear how to refine Eq. (3) because the reasons for the EC method's lack of closure (about 14% of the available net surface energy) are unknown. Provided that all the unexplained energy by the EC method in the surface energy balance arise from issues inherent in the EC method that are bypassed by the SRSE method (e.g., the need to account for detrending, shadowing, tilt correction, sensor separation and Reynolds decomposition among others), a refinement of Eq. (3) could be obtained by forcing closure of surface energy balance. In practice however, the latter likely would account for a portion of the available net surface energy balance that neither the EC nor the SRSE method can explain (e.g., fluxes associated to mean convection and mesoscale circulations). Further experiments are required to refine Eq. (3) over surfaces dominated by bare soil. However, here, the EC and SRSE methods performed comparably.

4.2 Discussion

By defining (as a rule of thumb) windy conditions when the mean (half-hourly) wind speed observed at Z = 3 m was, in general, higher than 1 m/s over a given period (i.e.,$(\bar{u} - \sigma_u) > 1\ \mathrm{m/s}$, where the overbar denotes average and σ_u is the standard deviation of the mean wind speed), it was observed throughout the campaign that windy conditions prevailed for the bare dataset and for the first 20 days of the sparse-canopy dataset. Lighter winds (i.e.,$(\bar{u} - \sigma_u) < 1\ \mathrm{m/s}$) and clear sky days were the prevailing atmospheric conditions for the last 10 days of the sparse - canopy dataset and for the entire homogeneous – canopy dataset. Calm conditions imply a lack of good ramp formation by shear in the traces and that the scalar exchange around midday under clear skies is dominated by large convective eddies. Both atmospheric conditions are compromising because a regular and well-defined canopy scale coherent motions are crucial for the SRSE method and large eddies are poorly sampled within a half-hourly basis. These factors may explain the higher portion of the unexplained available net surface energy by the EC method in the homogeneous dataset (Sakai et al., 2001).

Given the challenge for any approach to surface flux estimation to perform better than the EC method, the performance obtained by the FCL approach should be highlighted. Across the dataset, the FCL method had excellent closure, in fact, even slightly better than for the EC method. Throughout the campaign, the EC method was able to explain between 81% and 92% of the available net surface energy for the different surface types, and for all the data it was unable to explain 18% of the available net surface energy. Consistently (i.e., regardless of the surface), energy balance closure tests show that the R^2 coefficient for the EC method was between the values obtained with the two SRSE methods The amounts of unexplained energy by the EC method may be split into two distinct general source of errors: one related to the EC method that are bypassed using the SRSE method (i.e., SRSE does not require measurement of the wind field) and the other related to common issues that are not accounted for by both EC and SRSE methods. Currently, it is unknown how to quantify the portion of the total unexplained energy corresponding to each error's source. Consequently, it is difficult to assure that the sampling frequency really played a role in the SRSE method's results and future research is required. To confirm these findings, the post-field EC data requirements may play a role in its performance and energy balance closure.

Regardless, the FCL approach does not share instrumentation to estimate H and LE, and so it may be used to fill gaps in series of EC-derived flux estimates. In practice, the results in Table 1 allow recommending the FCL method using a sampling frequency of 10 Hz because the mean wind speed is not required as an input and it is convenient to use thicker thermocouples because they are more affordable and less prone to damage.

5. Conclusions

Combining the frameworks of transilient and Surface Renewal theories with the analysis of Small fluctuations in scalar traces, Eddies (the SRSE method), the Free Convection Limit (FCL) approach for estimating the sensible and latent heat fluxes was derived to avoid measurement of the wind speed. Along a full cotton growing season and taking as a reference the EC method operating at 20 Hz, it was found that the EC and FCL methods performed similarly when taking measurements in the inertial sub-layer.

Performance was especially strong during periods where the mean (half-hour) wind speeds measured at 3 m above the ground were about 1 m s^{-1} or higher. If stable conditions are not met, this study corroborates that FCL approaches may extend up to near neutral cases for surface types commonly encountered in croplands. The SRSE method did not show a dependency on the sampling frequency. Therefore, in practice, sensible heat flux estimates using the FCL approach operating at 10 Hz appear convenient to apply at the farm level and for studies involving large spatial scales, such as in the framework of remote sensing, because the use of thick thermocouples allow denser spatial coverage and low cost monitoring. Though further research is required (especially over surfaces with a high portion of bare soil and light winds), given that this study involved different surface types, here it is concluded that (1) the FCL approach for the SRSE method can be recommended for unstable cases to perform sensible heat flux and latent heat flux model calibration when the wind speed is not available, (2) it may be considered to fill gaps in half-hourly EC flux series and (3) appears to be a convenient approach to estimate the sensible heat flux.

Acknowledgments

This work was supported under project RTI2018-098693-B-C31 Ministerio de Ciencia, Economía y Universidades of Spain. Data collection and analysis was partially funded through the U.S. Geological Survey (USGS) under Cooperative Agreements G11AP20066 and G16AP00040 administered by the Arkansas Water Resources Center at the University of Arkansas; the United States Department of Agriculture (USDA), Natural Resources Conservation Service under Cooperative Agreement 68-7103-17-119, and the United States National Science Foundation (NSF) under Award 1752083. We acknowledge the assistance of Yin-Lin “Jack” Chiu and Bryant Fong in data collection and analysis. The views and conclusions contained in this document are those of the authors and do not represent the opinions or policies of the USGS, NSF, or USDA; mention of trade names or commercial products does not constitute endorsement by any entity.

References

Albertson, J. D., Parlange, M. B., Katul, G.G., Chu, C., Striker, H., Tyler, S., 1995. Sensible Heat Flux From Arid Regions: A Simple Flux-Variance Method. Water Resour. Res. 31(4). http://doi.org/10.1029/94WR02978.

Alfieri, J.G., Kustas, W.P., Prueger, J.H., Hipps, L.E., Evett, S.R., Basara, J.B., Neale, C.M.U., French, A.N., Colaizzi, P., Agam, N., Cosh, M.H., Chávez, J.L., Howell, T.A., 2012. Estimation of surface energy fluxes using surface renewal and flux variance techniques over an advective irrigated agricultural site. Adv. Water Resour. 50, 62-78.

Aminzadeh, M., Breitenstein, D., Or, D., 2017. Characteristics of Turbulent Airflow Deduced from Rapid Surface Thermal Fluctuations: An Infrared Surface Anemometer. Bound.-Lay. Meteorol. 165, 519–534. http://doi.org/10.1007/s10546-017-0279-5

Aubinet, M., Grelle, A., Ibrom, A., Rannik, Ü., Moncrieff, J., Foken, T., Kowalski, A.S., Martin, P.H., Berbigier, P., Bernhofer, C., Clemen,t R., Elbers, J., Granier, A., Grünwald, T., Morgenstern, K., Pilegaard, K., Rebmann, C., Snijders, W.,Valentini, R.,Vesala, T., 2000. Estimates of the annual net carbon and water exchange of forests: the EUROFLUX methodology. Adv Ecol Res. 30, 113–175.

Brunsell, N.A., Mechem, D.B., Anderson, M.C., 2011. Surface heterogeneity impacts on boundary layer dynamics via energy balance partitioning. Atmos. Chem. Phys. 11, 3403–3416.

Brutsaert, W., 1982. Evaporation into the Atmosphere. Environmental Fluid Mechanics. Kluwer Academic Publishers. Dordrecht/Boston/London (299 pp).

Burba, G., 2013. Eddy Covariance Method for Scientific, Industrial, Agricultural and

Regulatory Applications. LiCor Biosciences, Lincoln, Nebraska.

Castellví, F., 2018. An advanced method based on surface renewal theory to estimate the friction velocity and the surface heat flux. Water Resour. Res. 54. http://doi.org/10.1029/2018WR022808.

Castellví, F., Oliphant, A., 2017. Daytime sensible and latent heat flux estimates for a mountain meadow using in-situ slow-response measurements. Agr. Forest Meteorol. 236, 135–144.

Castellví, F., 2013. A method for estimating the sensible heat flux in the inertial sub-layer from high-frequency air temperature and averaged gradient measurements. Agr. Forest Meteorol. 180, 68-75.

Castellví, F., 2004. Combining surface renewal analysis and similarity theory: A new approach for estimating sensible heat flux. Water Resour. Res. 40, W05201. http://doi.org/10.1029/2003WR002677.

Charuchittipan, D., Babel, W., Mauder, M., Leps, J.P., Foken, T., 2014. Extension of the averaging time in eddy-covariance measurements and its effect on the energy balance closure. Bound.-Lay. Meteorol. 152 - 303. http://doi:10.1007/s10546-014-9922-6.

Chen, W., Novak, M.D., Black, T.A., Lee, X., 1997. Coherent eddies and temperature structure functions for three contrasting surfaces. Part I. Ramp model with finite micro-front time. Bound.-Lay. Meteorol. 84, 99-123.

Danckwerts, P., 1951. Significance of liquid-film coefficients in gas absorption. Ind. Eng. Chem. 43(6), 1460–1467.

De Bruin, H.A.R., Kohsiek, W., Vandenhurk, B.J.J.M., 1993. A verification of some methods to determine the fluxes of momentum, sensible heat, and water vapor using standard deviation and structure parameter of scalar meteorological quantities. Bound.-Lay. Meteorol. 63 (3), 231-257.

Dominguez, F., Kumar, P., Vivoni, E. R., 2008. Precipitation recycling variability and ecoclimatological stability—A study using NARR data. Part II: North American monsoon region. J. Climate. 21, 5187–5203.

Drexler, J. Z., Snyder, R. L., Spano, D., Paw U, K.T., 2004. A review of models and micrometeorological methods used to estimate wetland evapotranspiration. Hydrol. Process. 18, 2071–2101. http://doi: 10.1002/hyp.1462.

Drexler, J. Z., Anderson, F.E., Snyder, R. L., 2008. Evapotranspiration rates and crop coefficients for a restored marsh in the Sacramento–San Joaquin Delta, California, USA. Hydrol. Process. 22, 725–735. http://doi: 10.1002/hyp.6650.

Dyer, A.J., 1974. A review of flux-profile relationships. Bound.-Lay. Meteorol. 7, 363–372.

Eder, F., De Roo, F., Kohnert, K., Desjardins, R.L., Schmid, H.P., Mauder, M., 2014. Evaluation of two energy balance closure parametrizations. Bound.-Lay. Meteorol. 151, 195. http://doi.org/10.1007/s10546-013-9904-0

Higbie, R., 1935. The rate of absorption of a pure gas into a still liquid during short periods of exposure. Trans. AIChE, 31, 365–388.

Fang, L., Yang, J., White, M., Liu, Z., 2018. Predicting potential fire severity using vegetation, topography and surface moisture availability in a Eurasian Boreal Forest landscape. Forest. 9, 130. http://doi.org/10.3390/f9030130.

Foken, T., 2008. Micrometeorology. Springer-Verlag (Berlin – Heidelberg) Publishers, 306 pp.

Foken, T., Oncley, S.P., 1995. Workshop on instrumental and methodical problems of land surface flux measurements. Bull. Amer. Meteorol. Soc, 76, 1191–1193.

Foken, T., Aubinet, M., Finnigan, J.J., Leclerc, M.Y., Mauder, M., Paw U, K.T., 2011. Results of a panel discussion about the energy balance closure correction for trace gases. Bull. Am. Meteorol. Soc. 92, ES13–ES18. https://doi.org/10.1175/2011BAMS3130.1.

Fong, B., Reba, M.L., Teague, T.G., Runkle, B.R.K., Suvočarev, K., 2020, Eddy covariance measurements of carbon dioxide and water fluxes in US mid-south cotton production, Agric., Ecosyst. & Env., 292, 106813, https://doi.org/10.1016/j.agee.2019.106813.

French, A.N., Alfieri, J.G., Kustas, W.P., Prueger, J.H., Hipps, L.E., Chávez, J.L., Evett, S.R., Howell, T.A., Gowda, P.H., Hunsaker, D.J., Thorp, K.R., 2012. Estimation of surface energy fluxes using surface renewal and flux variance techniques over an advective irrigated agricultural site. Adv. Water Resour. 50, 91-105.

Fuchs, M., Tanner, C.B., 1968. Calibration and field test of soil heat flux plates. Soil Sci. Soc. Am.Proc. 32, 326–328.

Haghighi, E., Or, D., 2015. Linking evaporative fluxes from bare soil across surface viscous sublayer with the Monin–Obukhov atmospheric flux-profile estimates. J. Hydrol. 525, 684–693.

Haghighi E., Or, D., 2013. Evaporation from porous surfaces into turbulent airflows: coupling eddy characteristics with pore scale vapor diffusion. Water Resour. Res. 49, 8432–8442. http://doi:10.1002/2012WR013324.

Haymann, N., Lukyanova, V., Tanny, J., 2019. Effects of variable fetch and footprint on surface renewal measurements of sensible and latent heat fluxes in cotton. Agr. Forest Meteorol. 124, 237-251. http://doi.org/10.1016/j.agrformet.2019.01.010.

Horst, T.W., Semmer, S.R., Maclean, G., 2015. Correction of a Non-orthogonal, Three-Component Sonic Anemometer for Flow Distortion by Transducer Shadowing. Bound.-Lay. Meteorol. 155, 371–395. http://doi.org/10.1007/s10546-015-0010-3.

Hsieh, C-I., Katul, G.G., 1996. Estimation of momentum and heat fluxes using dissipation and flux variance methods in the unstable surface layer. Water Resour. Res. 32(8), 2453–2462.

Huang, J., Lee, X., Patton, E., 2008. A modelling study of flux imbalance and the influence of entrainment in the convective boundary layer. Bound.-Lay. Meteorol. 127, 273–292.

Kanda, M., Inagaki, A., Letzel, M.O., Raasch, S., Watanabe, T., 2004. LES Study of the energy imbalance problem with eddy covariance fluxes. Bound.-Lay. Meteorol. 110, 381–404.

Katul, G.G., Hsieh, C-I., Oren, R., Ellsworth, D., Philips, N., 1996. Latent and sensible heat flux predictions from a uniform pine forest using surface renewal and flux variance methods. Bound.-Lay. Meteorol. 80, 249-282.

Kohsiek, W., 1982. Measuring C_T^2, C_Q^2, and C_{TQ} in the unstable surface-layer, and relations to the vertical fluxes of heat and moisture. Bound.-Lay. Meteorol. 24(1), 89–107.

Monin, A.S., Yaglom, A.M., 1971. Statistical Fluid Mechanics: Mechanics of Turbulence. Vol. 1, The MIT Press, 782 pp.

Noltz, R., Krammerer, G., Cepuder, P., 2013. Interpretation of lysimeter weighing data affected by wind. Journal of Plant Nutrition and Soil Science, 176(2), 200-208.

Paw U., K.T, Qiu, J., Su, H-B., Watanabe, T., Brunet, Y., 1995. Surface renewal analysis: a new method to obtain scalar fluxes without velocity data. Agr. Forest Meteorol. 74, 119-137.

Robles-Morua, A., Vivoni, E.R., Mayer, A.S., 2012. Distributed Hydrologic Modeling in Northwest Mexico Reveals the Links between Runoff Mechanisms and Evapotranspiration. J. Hydrometeorol. 13, 785-805. http://doi.org/10.1175/JHM-D-11-0112.1.

Sakai, R., Fitzjarrald, D., Moore, K. E., 2001. Importance of low-frequency contributions to eddy fluxes observed over rough surfaces. J. Applied Meteorol. 40, 2178–2192.

Sauer, T.J., Horton, R., 2005. Soil heat flux. Chapter 7 in: J.L. Hatfield and J.M. Baker (Editors), Micrometeorology in agricultural systems. ASA Monograph 47: 131-154. American Society of Agronomy, Madison, Wisconsin. http://doi.org/10.2134/agronmonogr47.c7.

Schotanus, P., Nieuwstadt, F.T.M., DeBruin, H.A.R., 1983. Temperature measurement with a sonic anemometer and its application to heat and moisture fluctuations. Bound.-Lay. Meteorol. 26, 81-93.

Seo, Y.G., Lee, W.K., 1988. Single-eddy model for random surface renewal. Chem.Eng.Sci. 43(6), 1395–1402. http//doi.org/ 10.1016/0009-2509(88) 85112-1.

Shapland, T.M., McElrone, A.J., Snyder, R.L., Paw U, K.T., 2012. Structure function analysis of two-scale scalar ramps. Part I: theory and modelling. Bound.-Lay. Meteorol. 145, 5–25. http://doi.org/10.1007/s10546-012-9742-5.

Silva, D., Meza, F. J., Varas, E., 2010. Estimating reference evapotranspiration (ETo) using numerical weather forecast data in central Chile. J. Hydrol. 382, 64–71.

Snyder, R.L., Spano, D., Paw U, K.T., 1996. Surface renewal analysis for sensible and latent heat flux density. Bound.-Lay. Meteorol. 77, 249-266.

Stagl J., Mayr, E., Koch, H., Hattermann, F.F., Huang, S., 2014. Effects of Climate Change on the Hydrological Cycle in Central and Eastern Europe. In: Rannow S., Neubert M, eds. Managing Protected Areas in Central and Eastern Europe Under Climate Change. Advances in Global Change Research, vol 58. Springer, Dordrecht.

Steinfeld, G., Letzel, M., Raasch, S., Kanda, M., Inagaki, A., 2007. Spatial representativeness of single tower measurements and the imbalance problem with eddy-covariance fluxes: results of a large-eddy simulation study. Bound.-Lay. Meteorol. 123, 77–98.

Stoy, P.C., Mauder, M., Foken, T., Marcolla, B., Boegh, E., Ibrom, A., Arain, M.A., Arneth, A., Aurela, M., Bernhofer, C., Cescatti, A., Dellwik, E., Duce, P., Gianelle, D., van Gorsel, E., Kiely, G., Knohl, A., Margolis, H., McCaughey, H., Merbold, L., Montagnani, L., Papale, D., Reichstein, M., Saunders, M., Serrano-Ortiz, P., Sottocornola, M., Spano, D., Vaccari, F., Varlagin, A., 2013. A data-driven analysis of energy balance closure across FLUXNETresearch sites: the role of landscape scale heterogeneity. Agric For Meteorol. 171, 137–152.

Stoy, P.C., Katul, G.G., Siqueira, M.B.S., Juang, J.Y., Novick, K.A., McCarthy, H.R., Oishi, A.C., Uebelherr, J.M., Kim, H.S., Oren, R.A.M., 2006. Separating the effects of climate and vegetation on evapotranspiration along a successional chrono sequence in the southeastern US. Glob Change Biol. 12, 2115–2135.

Stull, R.B., 1988. An introduction to boundary layer meteorology. Kluwer, Dordrecht 666 pp.

Suvočarev, K., Castellví, F., Reba, M.L., Runkle, B.R.K., 2019. Surface renewal measurements of H, λE and CO2 fluxes over two different agricultural systems. Agr. Forest Meteorol. http://doi.org/10.1016/j.agrformet.2019.107763.

Twine, T.E., Kustas, W.P., Norman, J.M., Cook, D.R., Houser, P.R., Teyers, T.P., Prueger, J.H., Starks, P.J., Wesely, M.L., 2000. Correcting eddy-covariance flux underestimates over a grassland. Agr. Forest Meteorol. 103(3), 279-300

Wang, J., Brass, R.L., 2010. An Extremum Solution of the Monin–Obukhov Similarity Equations. J. Atmos. Sci. 785 - 499. http://doi.org/10.1175/2009JAS3117.1.

Li, P., Wang, Z.H., 2019. Estimating evapotranspiration over vegetated surfaces based on wet patch patterns. Hydrology Research, 50, 1037-1046.

Wilson, K., Goldstein, A., Falge, E., Aubinet, M., Baldocchi, D.D., Berbigier, P., Bernhofer, C., Ceulemans, R., Dolman, H., Field, C., Grelle, A., Ibrom, A., Law, B.E., Kowalski, A., Meyers, T.P., Moncrieff, J., Monson, R., Oechel, W., Tenhumen, J., Valentini, R., Verma, S., 2002. Energy balance closure at FLUXNET sites. Agric. For. Meteorol. 113, 223–143.

Yang, J., Wang, Z.H., 2014. Land surface energy partitioning revisited: A novel approach based on single depth soil measurement. Geophysical Research Letters, 41, 8348-8358.

Zapata, N., Martínez-Cob, A., 2001. Estimation of sensible and latent heat flux from natural sparse vegetation surfaces using surface renewal. J. Hydrol. 254, 215–228. http://doi.org/10.1016/S0022-1694(01)00495-4.

Zapata, N., Martínez-Cob, A., 2002. Evaluation of the surface renewal method to estimate wheat evapotranspiration. Agric. Water Manage. 55 (2), 141-157. http://doi.org/10.1016/S0378-3774(01)00188-3.

Zhao, X., Liu, Y., Tanaka, H., Hiyama, T., 2010. A comparison of flux variance and surface renewal methods with eddy covariance. IEEE Journal of selected topics in applied earth observations and remote sensing, 3 (3), 345-350.

Zhu, W., Van Hout, R., Katz, J., 2007. On the flow structure and turbulence during sweep and ejection events in a wind-tunnel model canopy. Bound.-Layer Meteor. 124, 205–233.

Table 1. Comparison of sensible heat and latent heat flux estimates using trace of scalars sampled at 10 Hz versus the corresponding EC results and the total eddy flux versus the available net surface energy for the bare, sparse - canopy and homogeneous – canopy datasets. N_s is the total number of samples available, s, int and R^2 are the slope, the intercept and the coefficient of determination of the linear regression analysis, respectively. NRMSE is the relative root mean square error and MBE is the mean bias error. In parentheses are the results using a sampling frequency of 20 Hz if different from 10 Hz.

Surface:	Bare soil dataset (N_s=1062, N^*=117)				
Comparison:	s	int (Wm^{-2})	R^2	NRMSE	MBE (Wm^{-2})
H_{Est} vs H_{EC}	1.24 (0.97)	10	0.82 (0.80)	0.72 (0.49)	-27 (-8)
H_{FCL} vs H_{EC}	1.26 (0.87)	2 (3)	0.90 (0.87)	0.56 (0.35)	-21 (5)
LE_{Est} vs LE_{EC}	1.02 (0.81)	9 (8)	0.83 (0.81)	0.45 (0.43)	-11 (13)
LE_{FCL} vs LE_{EC}	0.96 (0.82)	5 (4)	0.94 (0.93)	0.16 (0.25)	1 (24)
(H_{EC}+LE_{EC}) vs (Rn-G)*	0.86	9	0.84	0.32	-19
(H_{Est}+LE_{Est}) vs (Rn-G)*	0.85 (0.68)	9 (4)	0.75 (0.79)	0.42 (0.47)	-25 (-65)
(H_{FCL}+LE_{FCL}) vs (Rn-G)*	0.92 (0.76)	-2 (-3)	0.87 (0.94)	0.31 (0.36)	-21 (-58)
Surface:	Sparse - canopy dataset (N_s =609)				
H_{Est} vs H_{EC}	1.16 (0.89)	7 (9)	0.85 (0.80)	0.56 (0.44)	-15 (-4)
H_{FCL} vs H_{EC}	1.03 (0.70)	0 (2)	0.93 (0.92)	0.27 (0.42)	-1 (-12)
LE_{Est} vs LE_{EC}	1.12 (0.90)	2 (0)	0.92 (0.90)	0.31 (0.27)	-24 (19)
LE_{FCL} vs LE_{EC}	0.86 (0.78)	13 (11)	0.85	0.21 (0.27)	19 (33)
(H_{EC}+LE_{EC}) vs (Rn-G)	0.91	18	0.83	0.21	9
(H_{Est}+LE_{Est}) vs (Rn-G)	1.06 (0.91)	32 (20)	0.73 (0.71)	0.35 (0.31)	-45 (10)
(H_{FCL}+LE_{FCL}) vs (Rn-G)	0.98 (0.83)	-8 (-6)	0.95 (0.95)	0.12 (0.23)	13 (52)
Surface:	Homogeneous - canopy dataset (N_s =1703)				
H_{Est} vs H_{EC}	1.38 (1.07)	1 (4)	0.85 (0.81)	0.77 (0.52)	-20 (-7)
H_{FCL} vs H_{EC}	1.28 (0.88)	0 (1)	0.94 (0.93)	0.49 (0.27)	-13 (4)
LE_{Est} vs LE_{EC}	1.22 (0.96)	5 (4)	0.89 (0.88)	0.46 (0.28)	-41 (3)
LE_{FCL} vs LE_{EC}	1.08 (0.99)	6 (-1)	0.88	0.22 (0.18)	-23 (6)
(H_{EC}+LE_{EC}) vs (Rn-G)	0.80	14	0.87	0.24	52

(H_{Est}+LE_{Est}) vs (Rn-G)	1.00 (0.83)	46 (27)	0.72	0.35 (0.32)	-41 (29)
(H_{FCL}+LE_{FCL}) vs (Rn-G)	1.04 (0.89)	-12	0.96 (0.95)	0.11 (0.19)	0 (50)

Figure Captions

Figure 1. A descending cool and dry large parcel of air will remain in contact with the surface for a given period until, by continuity, it will be replaced by a fresh parcel of air (panel a). The signature of the coherent motion (a) in scalar traces at the measurement height is modelled by a large ramp-like shape (thick orange) as shown in panel b for the actual sonic temperature (T) change (thin black solid, left y-axis) and water vapor concentration (W) change (thin blue solid, right y-axis) with time. The large ramp-like shape is a composition of three phases (vertical dotted lines): a quiescent period, a gradually enriching (sensible heat and moisture) period and an ejection period (microfront). A population of fluid elements remain attached to the large-parcel ejected (a). These are identified by fluctuations embedded in the large ramp-like shape (b) whose signatures are modelled as a small ramp-like shape without quiescent period. This is shown in panel c, zoom of the green box (b), which identifies in the T trace (dotted black) two fluid elements (thick black) and one fluid element (thick blue) in the W trace (dotted blue line).

Figure 2. Comparison of (H_{EC}+LE_{EC}) (red circles) and (H_{FCL}+LE_{FCL}) determined using traces sampled at 10 Hz (blue crosses) versus (Rn-G) for all the data over a a) partly mulched bare soil, b) growing crop and c) mature crop cotton field. The 1:1 line (grey) and linear regression lines (blue, solid for 10 Hz; pink, solid for EC) are also shown.

Figure 1

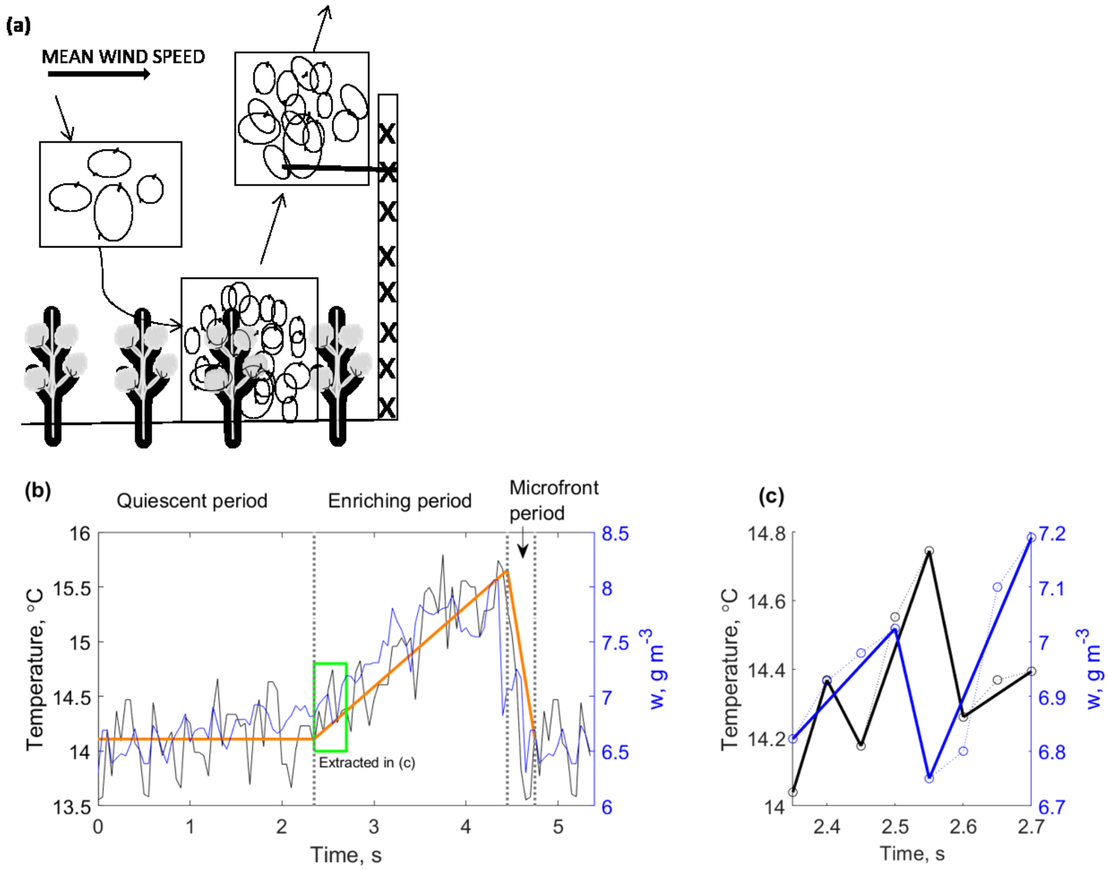

Figure 2